Nonstandard neutrino self-interactions can cause neutrino flavor equipartition inside the supernova core

Sajad Abbar

Max-Planck-Institut für Physik (Werner-Heisenberg-Institut), Föhringer Ring 6, 80805 München, Germany

(Received 29 August 2022; accepted 13 April 2023; published 2 May 2023)

We show that nonstandard neutrino self-interactions can lead to total flavor equipartition in a dense neutrino gas, such as those expected in core-collapse supernovae. In this first investigation of this phenomenon in the multiangle scenario, we demonstrate that such a flavor equipartition can occur on very short scales, and therefore very deep inside the newly formed proto-neutron star, with a possible significant impact on the physics of core-collapse supernovae. Our findings imply that future galactic core-collapse supernovae can appreciably probe nonstandard neutrino self-interactions, for certain cases even when they are many orders of magnitude smaller than the Standard Model terms.

DOI: 10.1103/PhysRevD.107.103002

I. INTRODUCTION

Core-collapse supernova (CCSN) explosions, caused by the death of massive stars, are among the most energetic astrophysical settings [1–4]. During the explosion, a huge amount of energy is released of which almost 99% is in the form of neutrinos of all flavors. Given the short duration of the burst, the number density of the neutrinos in such environments is so huge that the neutrino-neutrino interactions can play a crucial role in their flavor evolution [5–10].

In this paper, we study the impact of nonstandard neutrino self-interactions (νNSSI) on their flavor evolution in dense neutrino media. Such νNSSI are allowed in some of the beyond-the-Standard-Model (BSM) theories of particle physics [11,12]. While a BSM scaler mediator results in the presence of a trivial mass term of the form $\bar{\nu}_\xi \nu_\eta$ in the Lagrangian [13], a vector mediator leads to the effective Lagrangian $\mathcal{L}_{\rm eff} \supset G_{\rm F}[\mathsf{G}^{\alpha\beta}\bar{\nu}_\alpha\gamma^\mu\nu_\beta][\mathsf{G}^{\xi\eta}\bar{\nu}_\xi\gamma_\mu\nu_\eta]$, which is very similar to the neutrino-neutrino interaction Lagrangian of the SM except that it now allows for new interaction terms coupling neutrinos with different flavors via $\mathsf{G}^{\alpha\beta}$'s (see Ref. [14] for a discussion on how the effective single-particle Hamiltonian obtained from the Lagrangian can have a different structure). Needless to say, the SM can be recovered by setting $\mathsf{G}^{\alpha\beta} = \delta_{\alpha\beta}$. The nonstandard components of G are related to the vector mediator mass m_V and the coupling strength g_V, by $|\mathsf{G}^{\alpha\beta}| \propto g_V^2/m_V^2$.

The current constraints on νNSSI are rather weak and mostly model dependent, namely, $|\mathsf{G}^{\alpha\beta}|$ can be in general a couple of orders of magnitude larger than one (see, e.g., Fig. 1 of Ref. [15]). Though laboratory constraints are expectedly looser, stronger limits are feasible from the astrophysical neutrinos and the early Universe.

As for the constraints from laboratory processes, despite the fact that the number density of neutrinos is very low to allow for any direct detection of νNSSI, it can be indirectly probed by the measurements of other particle decays/interactions. Of particular interest is the measurement of the invisible width of the Z boson [16,17] (see also a nice improvement of this in Ref. [18]).

νNSSI can also impact the physics of the early Universe in a number of ways. For example, one can derive constraints on νNSSI by noting that if the mediator is light enough it could be in thermal equilibrium in the early Universe, which changes the number of relativistic degrees of freedom and thus it can be probed through big bang nucleosynthesis [19]. νNSSI can also affect cosmic neutrino background properties, meaning that it can be constrained via the cosmic microwave background through its temperature angular power spectra [20,21].

νNSSI can be constrained by the observation of high-energy cosmic neutrinos as well. This comes from the fact that high-energy neutrinos can be attenuated by their propagation in the cosmic neutrino background if νNSSI is strong enough [22–28]. Besides, CCSNe have also been considered as a probe of νNSSI [29–31].

In order to study the flavor evolution of neutrinos in the presence of νNSSI, we solve the Liouville–von Neumann equation ($c = \hbar = 1$) [32]

$$i d_t \varrho_{\mathbf{p}} = \left[\frac{\mathsf{U}\mathsf{M}^2\mathsf{U}^\dagger}{2E_\nu} + \mathsf{H}_{\rm m} + \mathsf{H}_{\nu\nu,\mathbf{p}}, \varrho_{\mathbf{p}}\right], \tag{1}$$

where $\mathbf{p}$ is the neutrino momentum, $E_\nu = |\mathbf{p}|$, $\mathbf{v} = \mathbf{p}/E_\nu$, and M^2 are the energy, velocity, and mass-squared matrix of the neutrino, respectively, and U is the Pontecorvo-Maki-Nakagawa-Sakata matrix. Moreover, $\mathsf{H}_{\rm m}$ is the contribution from the matter term which is proportional to the matter (electron) density [33,34], and $\mathsf{H}_{\nu\nu}$ is the neutrino potential stemming from the neutrino-neutrino forward scattering in the presence of νNSSI [35–39],

$$\mathsf{H}_{\nu\nu,\mathbf{p}} = \sqrt{2}G_{\rm F}\int \frac{{\rm d}^3p'}{(2\pi)^3}(1-\mathbf{v}\cdot\mathbf{v}')\{\mathsf{G}(\varrho_{\mathbf{p}'}-\bar{\varrho}_{\mathbf{p}'})\mathsf{G} + \mathsf{G}\,{\rm Tr}[(\varrho_{\mathbf{p}'}-\bar{\varrho}_{\mathbf{p}'})\mathsf{G}]\}, \tag{2}$$

where $\mathsf{G} = \mathsf{1}$ in the SM. The diagonal components of G constitute the flavor-preserving νNSSI, whereas the off-diagonal components show flavor-violating νNSSI.

The impact of νNSSI on the coherent scatterings of neutrinos in a dense neutrino gas was first addressed in Ref. [36], in a single-angle two-flavor scenario. It was then investigated further in Refs. [40,41] where a similar single-angle model was employed and it was shown that νNSSI can lead to flavor instabilities in both normal and inverted mass orderings. It was also particularly demonstrated that the flavor-violating νNSSI lead to spectral splits during the SN neutronization burst.

In this paper, we provide the first multiangle investigation of νNSSI in a dense neutrino gas (for multiangle investigations in the SM see, e.g., Refs. [42,43]). Our results suggest that some of the most important insights obtained in the single-angle scenarios (Sec. II A) should be artifacts of the limitations of such models. To be more specific, we show that the flavor-violating νNSSI can lead to flavor equipartition in a multiangle neutrino gas on scales determined by the neutrino number density (Sec. II B).

II. TWO-FLAVOR SCENARIO

To study the flavor evolution of neutrinos in the presence of νNSSI, we consider a neutrino gas in the two-flavor scenarios (ν_e and ν_x, with $x = \mu, \tau$, and their antiparticles) in which neutrinos are emitted uniformly with emission angles in the range $[-\vartheta_{\rm max}, \vartheta_{\rm max}]$. We then consider a number of examples in a single-energy single-angle one-dimensional (1D) gas, a single-energy multiangle 1D gas, a single-energy multiangle two-dimensional (2D) gas, and a multienergy multiangle 1D gas. These sorts of models have been extensively used in the literature (e.g., Ref. [44]). Also, as usual when studying collective neutrino oscillations, we ignore the matter potential by assuming that it is constant and can be rotated away by transforming into a corotating frame. Dropping the matter term is specifically motivated once one considers neutrino flavor evolution deep inside the proto-neutron star (PNS), where on short scales the neutrino gas and the ambient medium can be considered to be isotropic and homogenous to a very good degree. In addition, except for our single-energy single-angle model, here we assume that the strength of the weak interaction, defined as $\mu = \sqrt{2}G_{\rm F}n_{\nu_e}$, is constant, and the vacuum frequency is set to be $|\omega| = 1$ km^{-1} for the single-energy cases.

In the two-flavor scenario, the νNSSI matrix can be written as,

$$\mathsf{G} = \begin{bmatrix} 1+\gamma_{ee} & \gamma_{ex} \\ \gamma_{ex}^* & 1+\gamma_{xx} \end{bmatrix}. \tag{3}$$

Following Ref. [36], one can write the coupling matrix as

$$\mathsf{G} = \frac{1}{2}(g_0\mathsf{1} + \boldsymbol{g}\cdot\boldsymbol{\sigma}), \tag{4}$$

where $g_0 = 2+\gamma_{ee}+\gamma_{xx}$, $g_1 = 2{\rm Re}(\gamma_{ex})$, $g_2 = 2{\rm Im}(\gamma_{ex}^*)$, and $g_3 = \gamma_{ee}-\gamma_{xx}$, of which g_2 can be absorbed by a redefinition of the neutrino phases. Note that g_0 provides a measure of the overall strength of the (nonstandard) weak interactions. From now on, we set $g_0 = 2$ so that all of the other quantities are normalized by g_0. The coupling matrix can now be written as

$$\mathsf{G} = \begin{bmatrix} 1+g_3 & g_1 \\ g_1 & 1-g_3 \end{bmatrix}. \tag{5}$$

Here we assume that $|g_3| < 1$, so that the diagonal components of G are positive. This implies that one can always set g_0 in such a way that the contributions from νNSSI to the diagonal components have the same sign as those of the SM, as might be naively expected because the diagonal νNSSI contribution should be $\propto |g_V|^2$ and the sign should not depend on the phase of g_V (though we cannot exclude the possibility of the opposite). This is unlike in Ref. [40], where such a limitation was not considered and a number of noticeable phenomena were reported for the cases with $|g_3| > 1$.

A. Single-angle scenario

For the sake of comparison and in order to acquire some useful insight, here we first provide our results of the single-angle calculations where we assume that in our model all of the neutrino beams experience exactly the same flavor evolution. To be consistent with the previous works [36,40], we assume that the neutrino number density is decreasing as a function of the propagated distance such that $\mu = 3\times10^4\ (10/r)^4$ km^{-1}, motivated by the supernova physics. As indicated in the left and middle panels of Fig. 1, while for the normal mass ordering (NO) the final content of $\bar{\nu}_e$ remains mostly unaffected by the flavor-violating νNSSI, it can be almost completely depleted in

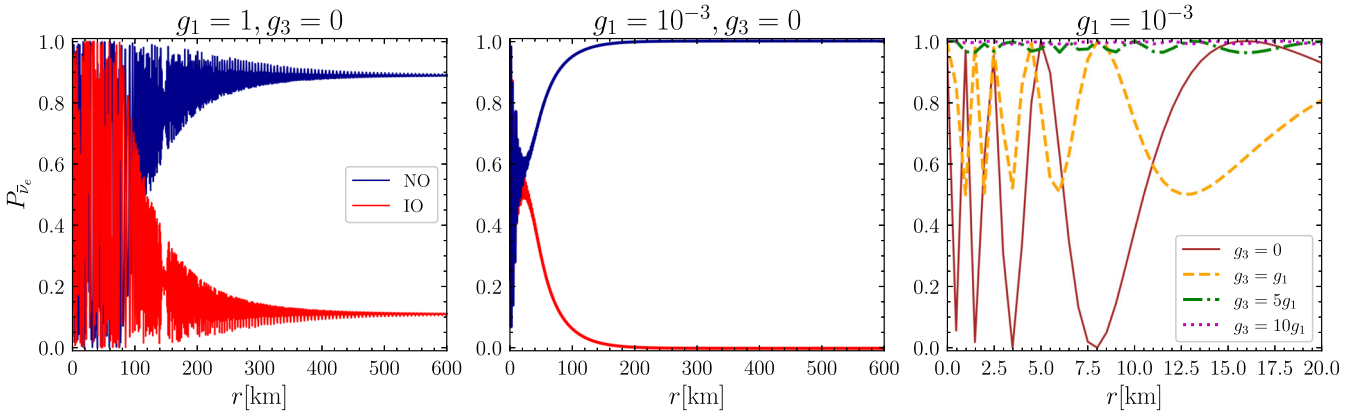

FIG. 1. Survival probabilities of $\bar{\nu}_e$ as a function of the propagated distance, for different values of g_1 and g_3, in our 1D model. The left and middle panels indicate that in the NO (IO) the flavor content of the neutrino gas is almost completely conserved (converted). On the other hand, the right panel shows the suppression caused by a nonzero g_3. Here we assume that $\mu = 3 \times 10^4\ (10/r)^4\ \mathrm{km}^{-1}$ and $n_{\bar{\nu}_e}/n_{\nu_e} = 0.8$.

the inverted mass ordering (IO). These results show a fantastic agreement with the results presented in Ref. [36], in spite of the difference between the geometries of the employed models.

The impact of nonzero flavor-preserving νNSSI is indicated in the right panel of Fig. 1. As can be clearly seen, the presence of a nonzero g_3 tends to suppress the flavor conversions once $g_3 \gtrsim g_1$. As discussed in the following, this insight (which was also pointed out in Ref. [40]) survives in the multiangle scenario.

B. Multiangle scenario

Having discussed the single-angle scenario, we now turn our focus to the multiangle simulations. As indicated in the left panel of Fig. 2, even very tiny flavor-violating νNSSI can lead to an almost perfect flavor equipartition on scales $\sim(g_1\mu)^{-1}$, as long as $g_1\mu \gtrsim 100\omega_{\mathrm{atm}}$. On the other hand, we have confirmed that 10% flavor conversions can be induced once $g_1\mu \sim 10\omega_{\mathrm{atm}}$.

Although the equipartition occurs in its complete form for $g_1 \gtrsim 0.5$, it holds on average for smaller g_1's where the average is taken over a few oscillations. As a matter of fact, what matters here is the ratio $\mathsf{H}_{\nu\nu}^{\text{off-diag}}/\mathsf{H}_{\nu\nu}^{\text{diag}}$. This can be better understood from the right panel of Fig. 2, which presents the angular distributions of ν_e survival probabilities for $g_1 = 0.1$ and 0.5, at $r \times g_1\mu = 30$. While the angular distribution of P_{ν_e} shows large amplitude modulations for $g_1 = 0.5$, the different angle beams are oscillating in phase for $g_1 = 0.1$. This explains the immediate flavor equipartition for $g_1 = 0.5$.

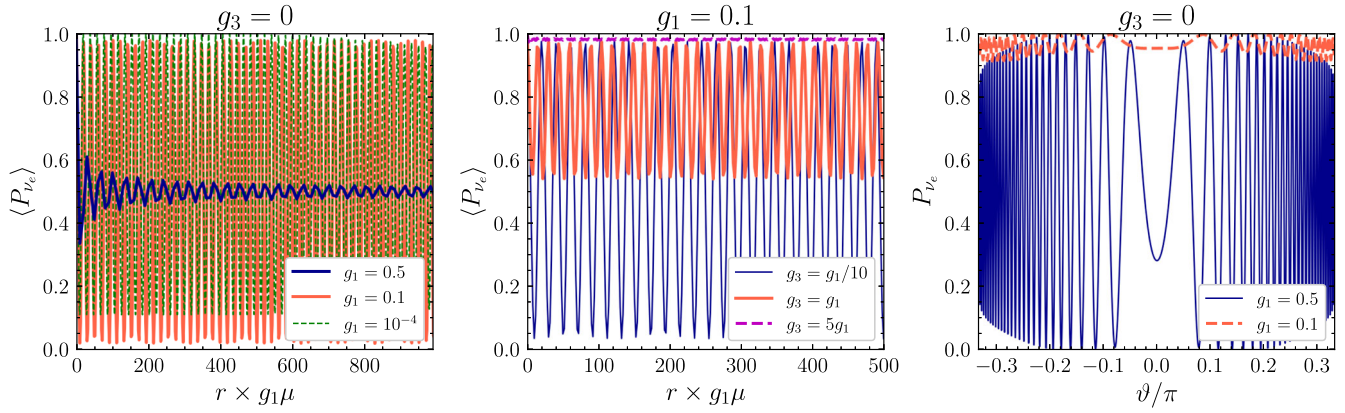

FIG. 2. Left and middle panels: angle-averaged survival probabilities of ν_e for different values of g_1 and g_3, in our 1D model. Although high values of g_3 can suppress flavor conversions (middle), the neutrino gas reaches flavor equipartition for a large enough g_1 (left). While for larger g_1's ($g_1 \gtrsim 0.5$) an exact flavor equipartition can be reached, it occurs in an average sense for smaller g_1's. Right panel: angular distributions of ν_e survival probabilities. Note that P_{ν_e} is quite uneven for $g_1 = 0.5$. Here we assume that $\mu = 10^6\ \mathrm{km}^{-1}$ and $n_{\bar{\nu}_e}/n_{\nu_e} = 0.8$. Although here and in all other calculations in this study we set $n_{\nu_x} = 0$, we have confirmed that the equipartition discussed here is not affected once $n_{\nu_x} \neq 0$. We have also confirmed that the results do not depend on the signs of g_1 and g_3 or the neutrino mass ordering.

In addition, nonzero flavor-preserving νNSSI can significantly suppress the flavor conversions provided that $g_3 \gtrsim g_1$, as demonstrated in the middle panel of Fig. 2. Note that this is consistent with the insight obtained in the single-angle scenario.

Although for smaller values of the flavor-violating νNSSI ($g_1 \lesssim 0.5$) the flavor equipartition occurs only on average in our 1D neutrino gas, the story could be different in multi-dimensional (MD) models. This is specifically plausible considering the fact that in an MD neutrino gas, each neutrino beam arriving at an arbitrary point (coming from different points on the source) should have already experienced a couple of large amplitude oscillations. Assuming that these beams have evolved somewhat independently, one should naively expect an exact equipartition in a multiangle MD neutrino gas even for smaller g_1's. This is illustrated clearly in Fig. 3, for a calculation in which $g_1 = 0.1$ and $g_3 = 0$. Here we consider a 2D (x and z) multiangle neutrino gas in which a periodic boundary condition is imposed along x, and the neutrino flavor evolution is followed along z. This model is similar to the one used in Refs. [45–47]. Although the neutrino gas experiences a few large amplitude oscillations initially, the coherence is lost afterwards and an almost perfect flavor equipartition is reached.

It is illuminating to note that the flavor equipartition discussed above (which is observed for $g_1 \gtrsim 0.5$ even in 1D models, but also observable for smaller g_1's in MD models) is purely a multiangle effect. Indeed, it occurs due to the occurrence of large amplitude modulations in the angular distributions of neutrinos.

Although the behavior observed in Fig. 3 is consistent with our insight that there should be an exact flavor equipartition in an MD gas, we alert the reader that we do not consider this topic as being settled since we could only run our 2D model simulations for very *few* points in the parameter space of μ-α-g_1 ($\alpha = n_{\bar{\nu}_e}/n_{\nu_e}$). This turns out to be indeed a very unstable problem from the numerical point of view and we postpone a thorough investigation of this effect to a future work.

The flavor equipartition discussed in this section is most relevant for the neutrino gas inside the PNS. This can be understood by considering the following observations. First, the PNS is the most sensitive zone to the νNSSI due to having the highest neutrino number densities. Hence, as long as $g_1\mu \gg \max(\omega, l_{\rm col}^{-1})$, the νNSSI-induced conversions can dominate the vacuum frequency oscillations and the collisional processes ($l_{\rm col}$ represents the collisional scales). In addition, if the neutrino gas is already in flavor equipartition at the neutrinosphere, then it should not change at larger radii (though we emphasize that this equipartition exists only in an average sense). One should also note that for such a problem which shows variations on very short scales and in which MD effects are important, 1D large-scale simulations, such as the one discussed in Fig. 1, should not be expected to provide very useful insights.

The flavor equipartition in the presence of νNSSI can even occur in the absence of vacuum mixing, i.e., once $\omega, \theta_{\rm V} = 0$, where $\theta_{\rm V}$ is the vacuum mixing angle. This is because the instability here arises solely from the flavor-violating νNSSI and has nothing to do with the vacuum mixing. To be more specific, the occurrence of flavor

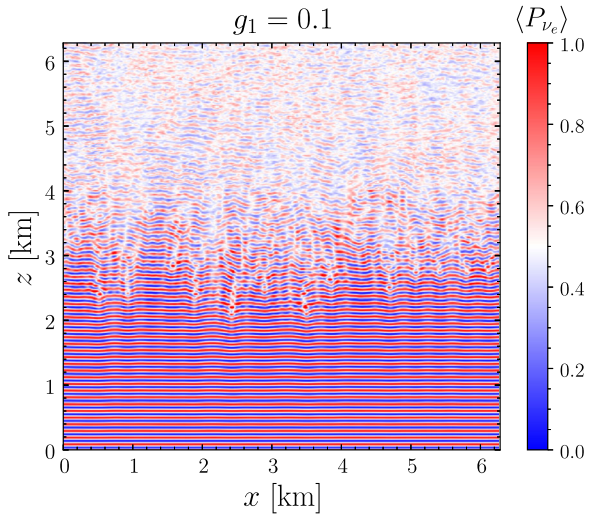

FIG. 3. Angle-averaged ν_e survival probability in our 2D single-energy multiangle model. The neutrino gas initially experiences a few large amplitude oscillations like what one observes in 1D calculations. The coherence is then lost and an almost perfect flavor equipartition is reached. Here we assume $g_1 = 0.1$, $g_3 = 0$, $\mu = 1000$ km^{-1}, and $n_{\bar{\nu}_e} = 0$ (a pure ν_e gas).

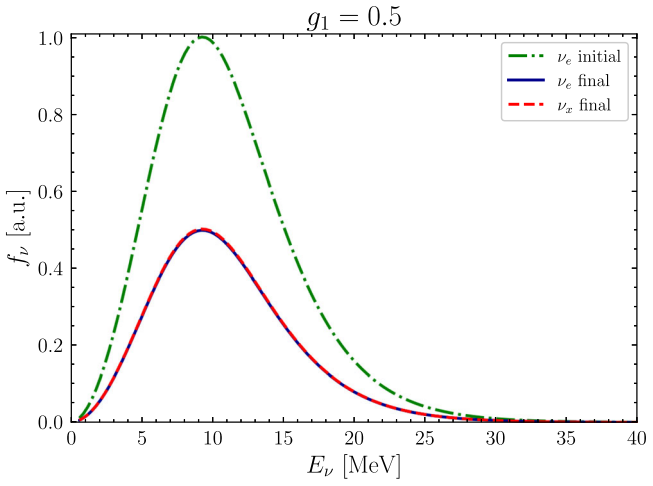

FIG. 4. Initial and final neutrino spectra of a neutrino gas which initially consists of a pure ν_e gas (appropriate during the neutronization burst) in the presence of νNSSI. As expected, the presence of flavor-violating νNSSI leads to a total flavor equipartition during the neutronization burst. Here we assume the initial neutrino gas to possess a Fermi-Dirac distribution equipped with a degeneracy parameter, though the choice of the initial spectra is arbitrary. Here we set $\mu = 10^6$ km^{-1}.

equipartition is not sensitive to ω (or the neutrino mass ordering) as long as $g_1\mu \gg |\omega|$.

One of the distinct results obtained in the single-angle scenario is the possibility of new spectral splits during the SN neutronization burst due to the presence of flavor-violating νNSSI [40]. This is particularly interesting given the fact that one normally does not expect collective oscillations during this phase (unless the matter profile is too shallow, as discussed in Refs. [48,49]). However, and as illustrated in Fig. 4, this behavior disappears in the multi-angle regime and instead one has total flavor equipartition between ν_e and ν_x, as expected from our discussions. Here we have considered a multiangle multienergy 1D model which initially consists of a pure ν_e gas. Needless to say, such an equipartition should be easier to measure given the fact that it should exist for all energy bins.

In the Appendix, we provide a simple intuitive understanding of the roles of g_1, g_3, and ω in flavor instabilities in the linear regime, which was previously missed in the literature.

III. CONCLUSION

We have studied neutrino flavor evolution in dense neutrino media in the presence of νNSSI in a multiangle model for the first time. We demonstrates that, although some of the insights obtained in the single-angle scenario also apply to the multiangle model, some others should be an artifact of the single-angle approximation. In particular, we showed that the dense neutrino gas can reach flavor equipartition on very short scales ($\sim g_1^{-1}\mu^{-1}$) in the presence νNSSI. We also illustrate that this effect can be suppressed by flavor-preserving component if $g_3 \gtrsim g_1$.

The νNSSI-induced flavor equipartition is of most relevance to the neutrino flavor evolution inside the PNS and the accretion disks of neutron star merger remnants. This simply comes from the fact that the neutrino number density is very high in such an environment. In addition, if neutrinos are already in flavor equipartition on the surface of the neutrino emitter, they might be expected to also maintain this equipartition at larger radii, unless something destroys it.

The equipartition caused by the νNSSI inside the PNS can have important observational and theoretical consequences. On the one hand, considering in particular the possible equipartition during the neutronization burst, one can probe g_1 down to values $g_1 \gtrsim 10^{-6}$. On the other hand, considering the high neutrino number densities expected inside the PNS ($n_\nu \sim 10^{36}$ cm^{-3}), the CCSN physics should be sensitive to $g_1 \gtrsim 10^{-8}$.

Although our study points out the interesting possibility of total flavor equipartition in a dense neutrino gas in the presence of νNSSI, it still has several important limitations. First, although equipartition as discussed in this work seems to be a robust phenomenon in the two-flavor scenario, the situation can be different in the three-flavor regime. In particular, this is expected considering the fact that in the three-flavor scenario there are more than one flavor-violating νNSSI parameters. Then, the expected equilibrium can in principle be different from equipartition. Second, the MD simulations of neutrino flavor evolution in the presence of νNSSI, as we also pointed out in the text, are highly prone to numerical instabilities. Although we could run a few simulations and we observed equipartition in MD models as presented in Fig. 3, a systematic exploration of MD effects remains to be addressed in a future work. In addition, neutrinos can also experience nonstandard interactions with matter (νNSI). Although such interactions are well constrained in model-dependent scenarios [50], the model-independent bounds are relatively loose [51]. The impact of νNSI on neutrino flavor evolution has been extensively studied for the neutrino gas above the PNS and accretion disks of neutron star merger remnants [14,52–55]. Considering the equipartition induced by νNSSI, one might then wonder if strong νNSI can also lead to equipartition inside the PNS.

ACKNOWLEDGMENTS

This work was supported by the German Research Foundation (DFG) through the Collaborative Research Centre "Neutrinos and Dark Matter in Astro- and Particle Physics (NDM)," Grant No. SFB-1258, and under Germany's Excellence Strategy through the Cluster of Excellence ORIGINS EXC-2094-390783311.

APPENDIX: LINEAR STABILITY ANALYSIS

In this appendix, we show that some of the insights developed in the nonlinear regime in the main text can be understood by linear stability analysis. For this purpose, we consider the simplest problem that can be solved analytically, i.e, a single-angle pure ν_e gas. Note that although such a single-angle model cannot provide us with any insight on flavor equipartition, it still can be very useful in understanding the roles of g_1, g_3, and ω in flavor instabilities.

In the linear regime, where the flavor conversion is still insignificant ($|\delta| \ll 1$), the neutrino density matrix can be written as

$$\rho = \begin{bmatrix} 1 & \delta \\ \delta^* & 0 \end{bmatrix}, \tag{A1}$$

with the total Hamiltonian being

$$\mathsf{H} = \frac{\omega}{2}\begin{bmatrix} 1 & 0 \\ 0 & -1 \end{bmatrix} + \mu[G\rho G + G\,\mathrm{Tr}(\rho G)], \tag{A2}$$

where here μ captures all of the information regarding the neutrino number density and the geometry.

Note that there is an important subtlety here: unlike the conventional flavor stability analysis, one *cannot* remove the trace of ρ in the presence of νNSSI. This is obvious given the fact that in the presence of νNSSI, the trace of ρ leads to a term $\propto G^2 + G\mathrm{Tr}(G)$ in the Hamiltonian, which is not necessarily benign to the stability analysis. In the linear regime (ignoring terms nonlinear in $|\delta|$), the equation of motion for δ then becomes

$$i\partial_t\delta = (\omega + 4\mu g_3^2 + 4\mu g_3 - 2\mu g_1^2)\delta - 2\mu g_1^2\delta^* - 2\mu g_1(1+g_3). \tag{A3}$$

This equation is very interesting in several aspects. First, there is a constant term which can be nonzero for nonzero g_1. This implies that for a large enough g_1, δ can experience a sudden enhancement on scales $\propto \mu^{-1}g_1^{-1}(1+g_3)^{-1}$. However, and although the right-hand side of Eq. (A3) is initially controlled by this term, it can eventually become subdominant once $|\delta|$ grows enough (though it might be already in the nonlinear regime).

In addition, Eq. (A3) couples δ to δ^*, which is different from the conventional linearized equation of motion for the flavor perturbations. This implies that the real and imaginary parts of δ can behave differently in the linear regime.

In order to get an impression of the stability of the neutrino gas in the presence of νNSSI, we assume that δ is already in a regime where the $2\mu g_1(1+g_3)$ term can be ignored. Then, one can find the following ordinary eigenvalue equation in terms of the real and imaginary components of δ:

$$\partial_t\begin{bmatrix}\delta_r\\ \delta_i\end{bmatrix} = \begin{bmatrix}0 & \eta\\ -\eta + 4\mu g_1^2 & 0\end{bmatrix}\begin{bmatrix}\delta_r\\ \delta_i\end{bmatrix}, \tag{A4}$$

where $\eta = \omega + 4\mu g_3^2 + 4\mu g_3$. The eigenvalues of this equation can be easily found to be

$$\lambda = \pm\sqrt{\eta(4\mu g_1^2 - \eta)}. \tag{A5}$$

Assuming $\eta > 0$, unstable solutions can only exist if $4\mu g_1^2 > \eta$, meaning that $g_1^2 > \omega/4\mu + g_3^2 + g_3$. This simple argument obviously shows the role of ω and g_3 in suppressing flavor instabilities discussed in the previous section, caused by the flavor-violating νNSSI. Note, however, that this is the insight obtained by ignoring the role of the $2\mu g_1(1+g_3)$ term, and after our understanding regarding the roles of g_1, g_3, and ω in the flavor instabilities. Otherwise, this simple argument has its own limitations, e.g., it fails when $\eta < 0$.

It should be kept in mind that the linear stability analysis presented here reaches very different results from the one in Ref. [41], given the following observations: (i) the trace of ρ is not removed in this study, as it should not be, and (ii) the $\mu g_1^2\delta^*$ term in the linearized equation of motion is the source of instability, meaning that one should not drop it in favor of the other terms. Then, for example, here we observe that the neutrino gas is always unstable as long as $g_1 \gtrsim g_3$, which is different from the results presented, e.g., in Fig. 1 of Ref. [41].

[1] S. A. Colgate and R. H. White, The hydrodynamic behavior of supernovae explosions, Astrophys. J. **143**, 626 (1966).
[2] H. A. Bethe and J. R. Wilson, Revival of a stalled supernova shock by neutrino heating, Astrophys. J. **295**, 14 (1985).
[3] H.-T. Janka, Explosion mechanisms of core-collapse supernovae, Annu. Rev. Nucl. Part. Sci. **62**, 407 (2012).
[4] A. Burrows, Colloquium: Perspectives on core-collapse supernova theory, Rev. Mod. Phys. **85**, 245 (2013).
[5] Y. Z. Qian and S. E. Woosley, Nucleosynthesis in neutrino driven winds: 1. The physical conditions, Astrophys. J. **471**, 331 (1996).
[6] S. Pastor and G. Raffelt, Flavor Oscillations in the Supernova Hot Bubble Region: Nonlinear Effects of Neutrino Background, Phys. Rev. Lett. **89**, 191101 (2002).
[7] H. Duan, G. M. Fuller, J. Carlson, and Y.-Z. Qian, Simulation of coherent non-linear neutrino flavor transformation in the supernova environment. 1. Correlated neutrino trajectories, Phys. Rev. D **74**, 105014 (2006).
[8] H. Duan, G. M. Fuller, J. Carlson, and Y.-Z. Qian, Coherent Development of Neutrino Flavor in the Supernova Environment, Phys. Rev. Lett. **97**, 241101 (2006).
[9] H. Duan, G. M. Fuller, and Y.-Z. Qian, Collective neutrino oscillations, Annu. Rev. Nucl. Part. Sci. **60**, 569 (2010).
[10] S. Chakraborty, R. Hansen, I. Izaguirre, and G. Raffelt, Collective neutrino flavor conversion: Recent developments, Nucl. Phys. **B908**, 366 (2016).
[11] Z. Bialynicka-Birula, Do neutrinos interact between themselves?, Nuovo Cimento **33**, 1484 (1964).
[12] D. Y. Bardin, S. M. Bilenky, and B. Pontecorvo, On the nu—nu interaction, Phys. Lett. **32B**, 121 (1970).
[13] S.-F. Ge and S. J. Parke, Scalar Nonstandard Interactions in Neutrino Oscillation, Phys. Rev. Lett. **122**, 211801 (2019).
[14] Y. Yang and J. P. Kneller, Neutrino flavor transformation in supernovae as a probe for nonstandard neutrino-scalar interactions, Phys. Rev. D **97**, 103018 (2018).

[15] J. M. Berryman *et al.*, Neutrino self-interactions: A white paper, in *2022 Snowmass Summer Study* (2022), arXiv:2203.01955.

[16] M. S. Bilenky, S. M. Bilenky, and A. Santamaria, Invisible width of the Z boson and "secret" neutrino-neutrino interactions, Phys. Lett. B **301**, 287 (1993).

[17] M. S. Bilenky and A. Santamaria, Bounding effective operators at the one loop level: The case of four fermion neutrino interactions, Phys. Lett. B **336**, 91 (1994).

[18] V. Brdar, M. Lindner, S. Vogl, and X.-J. Xu, Revisiting neutrino self-interaction constraints from Z and τ decays, Phys. Rev. D **101**, 115001 (2020).

[19] B. Ahlgren, T. Ohlsson, and S. Zhou, Comment on "Is Dark Matter with Long-Range Interactions a Solution to All Small-Scale Problems of Λ Cold Dark Matter Cosmology?", Phys. Rev. Lett. **111**, 199001 (2013).

[20] M. Archidiacono and S. Hannestad, Updated constraints on non-standard neutrino interactions from Planck, J. Cosmol. Astropart. Phys. 07 (2014) 046.

[21] F.-Y. Cyr-Racine and K. Sigurdson, Limits on neutrino-neutrino scattering in the early universe, Phys. Rev. D **90**, 123533 (2014).

[22] I. Esteban, S. Pandey, V. Brdar, and J. F. Beacom, Probing secret interactions of astrophysical neutrinos in the high-statistics era, Phys. Rev. D **104**, 123014 (2021).

[23] K. Ioka and K. Murase, IceCube PeV–EeV neutrinos and secret interactions of neutrinos, Prog. Theor. Exp. Phys. **2014**, 061E01 (2014).

[24] K. C. Y. Ng and J. F. Beacom, Cosmic neutrino cascades from secret neutrino interactions, Phys. Rev. D **90**, 065035 (2014); Phys. Rev. D **90**, 089904(E) (2014).

[25] M. Ibe and K. Kaneta, Cosmic neutrino background absorption line in the neutrino spectrum at IceCube, Phys. Rev. D **90**, 053011 (2014).

[26] K. Blum, A. Hook, and K. Murase, High energy neutrino telescopes as a probe of the neutrino mass mechanism, arXiv:1408.3799.

[27] A. DiFranzo and D. Hooper, Searching for MeV-scale gauge bosons with IceCube, Phys. Rev. D **92**, 095007 (2015).

[28] I. M. Shoemaker and K. Murase, Probing BSM neutrino physics with flavor and spectral distortions: Prospects for future high-energy neutrino telescopes, Phys. Rev. D **93**, 085004 (2016).

[29] E. W. Kolb and M. S. Turner, Supernova SN 1987A and the secret interactions of neutrinos, Phys. Rev. D **36**, 2895 (1987).

[30] S. Shalgar, I. Tamborra, and M. Bustamante, Core-collapse supernovae stymie secret neutrino interactions, Phys. Rev. D **103**, 123008 (2021).

[31] P.-W. Chang, I. Esteban, J. F. Beacom, T. A. Thompson, and C. M. Hirata, Towards powerful probes of neutrino self-interactions in supernovae, arXiv:2206.12426.

[32] G. Sigl and G. Raffelt, General kinetic description of relativistic mixed neutrinos, Nucl. Phys. **B406**, 423 (1993).

[33] L. Wolfenstein, Neutrino oscillations in matter, Phys. Rev. D **17**, 2369 (1978).

[34] S. P. Mikheyev and A. Yu. Smirnov, Resonance amplification of oscillations in matter and spectroscopy of solar neutrinos, Sov. J. Nucl. Phys. **42**, 913 (1985).

[35] G. Sigl and G. Raffelt, General kinetic description of relativistic mixed neutrinos, Nucl. Phys. **B406**, 423 (1993).

[36] M. Blennow, A. Mirizzi, and P. D. Serpico, Nonstandard neutrino-neutrino refractive effects in dense neutrino gases, Phys. Rev. D **78**, 113004 (2008).

[37] G. M. Fuller, R. W. Mayle, J. R. Wilson, and D. N. Schramm, Resonant neutrino oscillations and stellar collapse, Astrophys. J. **322**, 795 (1987).

[38] J. T. Pantaleone, Dirac neutrinos in dense matter, Phys. Rev. D **46**, 510 (1992).

[39] D. Nötzold and G. Raffelt, Neutrono dispersion at finite temperature and density, Nucl. Phys. **B307**, 924 (1988).

[40] A. Das, A. Dighe, and M. Sen, New effects of non-standard self-interactions of neutrinos in a supernova, J. Cosmol. Astropart. Phys. 05 (2017) 051.

[41] A. Dighe and M. Sen, Nonstandard neutrino self-interactions in a supernova and fast flavor conversions, Phys. Rev. D **97**, 043011 (2018).

[42] S. Chakraborty, T. Fischer, A. Mirizzi, N. Saviano, and R. Tomas, No Collective Neutrino Flavor Conversions During the Supernova Accretion Phase, Phys. Rev. Lett. **107**, 151101 (2011).

[43] A. Esteban-Pretel, S. Pastor, R. Tomas, G. G. Raffelt, and G. Sigl, Decoherence in supernova neutrino transformations suppressed by deleptonization, Phys. Rev. D **76**, 125018 (2007).

[44] S. Abbar and M. C. Volpe, On fast neutrino flavor conversion modes in the nonlinear regime, Phys. Lett. B **790**, 545 (2019).

[45] S. Abbar, H. Duan, and S. Shalgar, Flavor instabilities in the multiangle neutrino line model, Phys. Rev. D **92**, 065019 (2015).

[46] J. D. Martin, S. Abbar, and H. Duan, Nonlinear flavor development of a two-dimensional neutrino gas, Phys. Rev. D **100**, 023016 (2019).

[47] S. Abbar, Turbulence fingerprint on collective oscillations of supernova neutrinos, Phys. Rev. D **103**, 045014 (2021).

[48] H. Duan, G. M. Fuller, J. Carlson, and Y.-Z. Qian, Flavor Evolution of the Neutronization Neutrino Burst from an O-Ne-Mg Core-Collapse Supernova, Phys. Rev. Lett. **100**, 021101 (2008).

[49] B. Dasgupta, A. Dighe, A. Mirizzi, and G. G. Raffelt, Spectral split in prompt supernova neutrino burst: Analytic three-flavor treatment, Phys. Rev. D **77**, 113007 (2008).

[50] P. S. Bhupal Dev *et al.*, Neutrino non-standard interactions: A status report, SciPost Phys. Proc. **2**, 001 (2019).

[51] C. Biggio, M. Blennow, and E. Fernandez-Martinez, General bounds on non-standard neutrino interactions, J. High Energy Phys. 08 (**2009**) 090.

[52] C. J. Stapleford, D. J. Väänänen, J. P. Kneller, G. C. McLaughlin, and B. T. Shapiro, Nonstandard neutrino interactions in supernovae, Phys. Rev. D **94**, 093007 (2016).

[53] A. Chatelain and M. C. Volpe, Neutrino propagation in binary neutron star mergers in presence of nonstandard interactions, Phys. Rev. D **97**, 023014 (2018).

[54] K. S. Babu, G. Chauhan, and P. S. Bhupal Dev, Neutrino nonstandard interactions via light scalars in the Earth, Sun, supernovae, and the early Universe, Phys. Rev. D **101**, 095029 (2020).

[55] G. L. Fogli, E. Lisi, A. Mirizzi, and D. Montanino, Revisiting nonstandard interaction effects on supernova neutrino flavor oscillations, Phys. Rev. D **66**, 013009 (2002).